Laser and Particle Beams (2007), *25*, 23–30. Printed in the USA.

DOI: 10.1017/S0263034607070048

Radiation effects on shock propagation in Al target relevant to equation of state measurements

T. DESAI,[1,2] R. DEZULIAN,[1] AND D. BATANI[1]

[1]Dipartimento di Fisica "G.Occhialini," Università di Milano-Bicocca, Milano, Italy
[2]ETSII, Universidad Politecnica, Madrid, Spain

(RECEIVED 11 January 2006; ACCEPTED 25 August 2006)

Abstract

We present one-dimensional simulations performed using the multi group radiation hydro code MULTI with the goal of analyzing the target preheating effect under conditions similar to those of recent experiments aimed at studying the Equation of State (EOS) of various materials. In such experiments, aluminum is often used as reference material; therefore its behavior under strong shock compression and high-intensity laser irradiation (10^{13}–10^{14} W/cm^2) should be studied in detail. Our results reveal that at high laser irradiance, the laser energy available to induce shock pressure is reduced due to high X-rays generation. Simultaneously X-rays preheat the bulk of the reference material causing significant heating prior to shock propagation. Such effects induce deviations in shock propagation with respect to cold aluminum.

Keywords: Equation of state of matter; Preheating; Shock velocity; X-radiation effect

INTRODUCTION

One of the important applications of high power laser systems is the generation of high-pressure shocks for studying the equation of state (EOS) of matter. This study has significance in various branches of physics including condensed matter, astrophysics, planetology, fusion plasmas, and others. The usual method of measuring the EOS of material by the impedance matching technique is indeed classical and has been in vogue for almost 50 years (Al'tshuler *et al*., 1958*a*). In the recent years, high-quality shocks have been produced with laser irradiation by adopting optical smoothing techniques (Koenig *et al*., 1994; Batani *et al*., 1996, 2002); this has also allowed the pressure ceiling of EOS experiments to be considerably lifted, up to the 100 Mbar range (Batani *et al*., 2000).

The target configuration involving EOS measurements usually consists of Al base, a step of Al as the reference material, and another step of the *test* material (see Fig. 1). Al has been well accepted as a reference material and used routinely to study the EOS of other materials (Batani *et al*., 2003*a*, 2004; Koenig *et al*., 1995) and the SESAME table (Lyon & Johnson, 1992). Here the experimentally measurable parameter of the shock wave is the velocity of propagation (D) of the shock front, which is determined by measuring the shock transit time in the step. Hence, such target configuration allows the direct measurement of the shock velocity in the two materials *on the same* laser shot. This is a direct measurement. Since the EOS of the reference material is assumed to be known, the determination of D allows getting all the other shock parameters. Finally, by applying the calibrated reflection method (impedance mismatch technique), the shock pressure and the fluid velocity in the test material are then derived (Zeldovich & Raizer, 1967). Hence the reliability of EOS data relies on the behavior of the reference material.

However, in principle, laser-shock EOS experiments may be affected by target preheating due to the intense flux of X-rays produced in the plasma-corona. X-ray absorption in the reference and test materials leads to heating of the material before the arrival of the shock wave. Shock wave propagation in an X-ray preheated medium has been in discussion for the past 10 years and the topic is becoming more vital due to the increase in precision of EOS data obtained with laser driven shocks. This implies that while preheating-induced errors could often be considered negligible in first measurements, which were anyway characterized by large error bars, they may not be negligible in future experiments. Therefore, it becomes increasingly important to study and characterize the effects of preheating.

Address correspondence to T. Desai, Dipartimento di Fisica "G.Occhialini", Università di Milano-Bicocca, Milano-20126, Italy. E-Mail: Tara.Desai@mib.infn.it

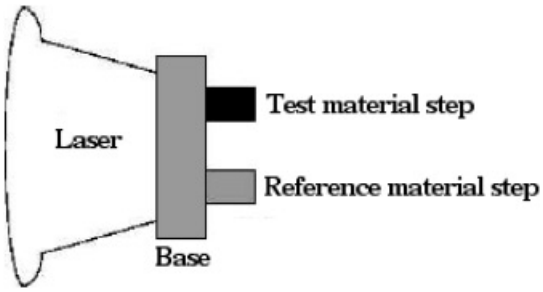

Fig. 1. Sketch of the configuration of a two-step target for EOS measurements. Base and reference steps are made of aluminum.

Propagation of the shock wave in an X-ray preheated medium involves several simultaneous processes. These include the impact of X-ray generation on shock pressure in Al target (which is a reference material for EOS) and changes in shock velocity due to target rear side expansion.

In order to reduce preheating effects, usually a plastic (CH) ablator is used on the laser-irradiated side (Koenig *et al*., 1995; Benuzzi *et al*., 1998; Batani *et al*., 2003*b*). Due to the lower atomic number of plastics components with respect to Al, the total X-ray yield is reduced and also softer (that is, less penetrating) X-rays are generated which cannot preheat the material in depth. Nevertheless, the presence of a CH layer complicates the situation by adding impedance mismatch effects on shock (and relaxation waves) propagation at the CH/Al interface. Therefore, we think that, before discussing the complications of a double (CH/Al) layer target, it is useful to try to understand what takes place in a simpler physical situation. Moreover, various aspects of the physics taking place in the reference material (Al) were never explicitly discussed before in the literature.

This paper complements previous works on the subject (Honrubia *et al*., 1998, 1999), which addressed the preheating problem in simple planar targets. They showed that target expansion on rear side always resulted in a delayed shock breakout. In laser-shock EOS experiments, the key parameter to be measured is the shock velocity, which is measured through the shock transit time in a stepped target, that is, as the difference of shock breakout times at the rear side of the base of the target and at the rear side of the step. Therefore, there is a delicate balance of various factors (which we'll describe in this paper) which introduced new interesting features with respect to the case of simple planar targets, and which were not discussed in previous works. Moreover, as already said, we explicitly discuss the reduction in shock pressure as a consequence of X-ray generation, which was not discussed in previous works.

Indeed, although the X-ray flux is generally lower in the steps as compared to the base (the base effectively acts as an absorber for the incident X-ray radiation), the steps usually allow a longer time for interaction. Hence, depending on the detailed target design (materials and thickness), the developments of preheat effects in the step (as well as in the base), and their impact on the shock propagation may be very important. Of course, as we already said, this is not really the situation met in real experiments. For instance, experimentalists do take care of not using too-high laser irradiance, and/or of adding a plastic layer (ablator) before the Al base on the laser irradiation side. Thus, very low preheat temperatures can be generated in Al, which are expected to produce only small effects. However, since one of the main goals of present-day laser-driven EOS experiments is the reduction of error bars (improvement of the reliability and accuracy of obtained data), even low-preheating level may have some effects. We recall that a *very low* preheating temperature of 0.1 eV is comparable or higher than the melting temperature of most solid materials. In any case, the work presented here deals with Al only. Results of the present work will be an important input to the future work where one can explicitly consider the effect of introducing a low-Z ablator layer, and the effects of preheating on the reference, and the test material *simultaneously*.

EXPERIMENTAL SET-UP

The typical scheme of present-day laser-driven EOS experiment is shown in Figure 1, and it is based on the generation of high quality shocks by using optical smoothing techniques like phase zone plates (Koenig *et al*., 1994; Batani *et al*., 1996, 2002), and on the use of *two steps − two materials* targets.

For instance, we consider as a reference, a recent experiment for the determination of carbon EOS points performed using the Prague asterix laser system (PALS) of wavelength $\lambda = 0.44\ \mu$m and pulse duration $\tau = 0.45$ ns (FWHM) focused on target at an intensity $< 1.5 \times 10^{14}$ W/cm^2 (Batani *et al*., 2004). Here the thickness of the base Al and step targets were 8 μm and 8.5 μm, respectively. Let's notice that at higher laser irradiance, the shock wave becomes non-stationary in the 8.5 μm Al layer used as step (Batani *et al*., 2000).

EXPERIMENTAL METHOD FOR EOS DETERMINATION:

When high-intensity laser radiation is focused on the front surface of the Al target base, an intense shock is generated and propagates inward. In the experiments, the appearance of the shock luminosity is the signature of the shock arrival at the rear surface of the target. The optical signals of the shock arrival on the rear surface of the base and the steps of the target are recorded using a streak camera. The interval between the shock breakout signal at the base (t_b) and at the step (t_s) provides the shock transit time in the step $\Delta t = (t_s - t_b)$. The experimental value of the shock velocity D is calculated as $D = d/\Delta t$, where d is the step target thickness. The shock fluid velocity U in Al is then determined using an EOS model, for instance, the well-known SESAME tables (Lyon & Johnson, 1992) or the MPQeos model (More *et al*.,

https://doi.org/10.1017/S0263034607070048 Published online by Cambridge University Press

1988; Kemp & Meyer-ter-Vehn, 1998). Usually these correspond to a linear relationship between D and U. For instance, in the few megabar pressure range, such a relation is $D = 6.08 + 1.21$ U from the SESAME tables, where D and U are in units of km/s, while it is $D = 5.76 + 1.23$ U from MPQeos. The first constant corresponds to the sound velocity in the material.

The shock pressure is then found by using one of the Hugoniot–Rankine relations, that is, $P = P_o + \rho_o DU$, where P_o and ρ_o are, respectively, the standard pressure and normal density of the un-shocked material.

The EOS point for the test material is finally found by using the experimental value of the shock velocity measured in the step of the test material, and by applying the impedance mismatch technique, as described in Zeldovich and Raizer (1967) and Batani *et al*. (2000).

SIMULATION MODEL:

In order to investigate the effect of X-ray radiation on the shock propagation, a relative study in comparison with an ideal cold medium is necessary. Therefore, simulations were performed: (1) in a realistic case, where the Al target generates and subsequently absorbs X-rays (*Radiative* case) and (2) by artificially suppressing X-ray emission and propagation (*Non radiative* case).

Simulations have been carried out with the one-dimensional (1D) radiation-hydrodynamic code MULTI (Ramis *et al*., 1988). This code uses the SESAME equation of state and the SNOP opacities (Eidmann, 1994). The particularity of this code, which makes it useful for performing this kind of study, is the possibility to switch the radiation transport off and then perform purely hydrodynamical simulations.

It is known (Honrubia *et al*., 1998, 1999) that, in our experimental conditions, preheating is mainly due to the photons generated in the corona with energies close to the Al K-edge ($h\nu \sim 1.5$ keV). At those energies, opacities are low and photons can propagate inward and preheat the base, reference and test materials steps.

It must also be noticed that, when we refer to experimental results, the laser intensity is known only to some degrees of approximation. Indeed, even if laser energy and laser pulse duration are measured shot by shot, the real laser intensity on target may differ from the value inferred by the measurements of the pulse energy and the pulse duration, due to the experimental uncertainties and the fluctuations related to these two quantities, to fluctuations in the focal spot and to the laser-plasma interaction processes (refraction in the plasma corona, non-linear parametric instabilities, etc.). For this reason, in comparing 1D simulations to the experimental results, one generally adjusts the laser intensities in the simulations in such a way to obtain shock transit times that match the experimental values. Of course, one expects the two intensity values (measured and simulated) to be roughly the same; if this is not the case, then the particular experimental shot should be questioned and carefully checked

RESULTS AND DISCUSSION

We have performed simulations between 2×10^{13} and 1.5×10^{14} W/cm^2 (in a few cases, we started the simulations at a lower minimum intensity value, that is, 0.5×10^{13} W/cm^2, in order to better understand the behavior of the involved quantities, Figs. 4, 6, and 7). The regime below our lower limit is not of great interest for very-high-pressure EOS experiments; on the other side, for I $> 1.5 \times 10^{14}$ W/cm^2, the shock wave becomes non-stationary in the step (Batani *et al*., 2003*a*) and severe preheating effects cannot be avoided due to the larger X-ray yield but also to the generation of hot electrons.

First, we study by simulation the development of preheating temperature of the rear surfaces of the Al base and step of the target as a function of time and laser intensity. Figure 2 shows the evolution of preheats at different times at 10^{14} and 1.35×10^{14} W/cm^2. Each curve stops just before the shock breakout at the (corresponding) rear surface. After this, temperature rises sharply due to shock break out.

Figure 3 shows instead the behavior of the "*maximum*" preheating temperature (that is, the temperature just before shock breakout) at the base and at the step, as a function of laser intensity. Interpolation curves are drawn by taking into account that the preheating temperature must reduce to the standard room temperature (0.025 eV) as laser intensity goes to zero. We see that preheat on both surfaces increases with increasing intensity. Figs. 2 and 3 clearly show that the shock wave propagates in a preheated medium.

Figure 4 shows instead the rear side expansion from the Al base and step as a function of laser intensity. This is the

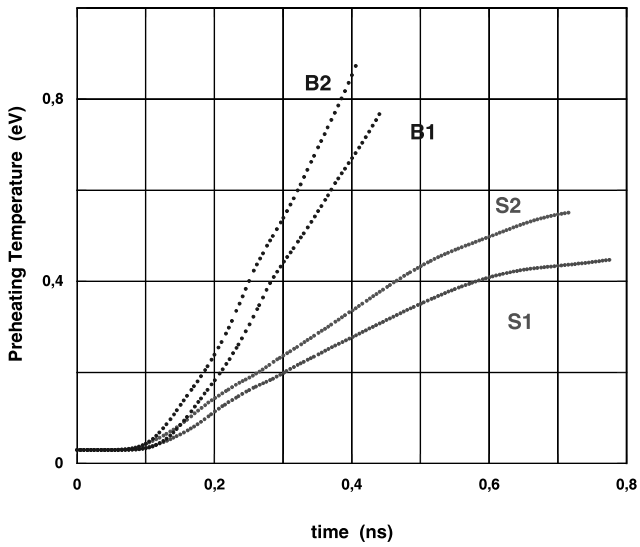

Fig. 2. Preheating temperature development with time at the rear surface of the 8 μm base (B1, B2) and 8.5 μm (S1,S2) for a laser intensity $\approx 10^{14}$ W/cm^2 and $\approx 1.35 \times 10^{14}$ W/cm^2, respectively.

https://doi.org/10.1017/S0263034607070048 Published online by Cambridge University Press

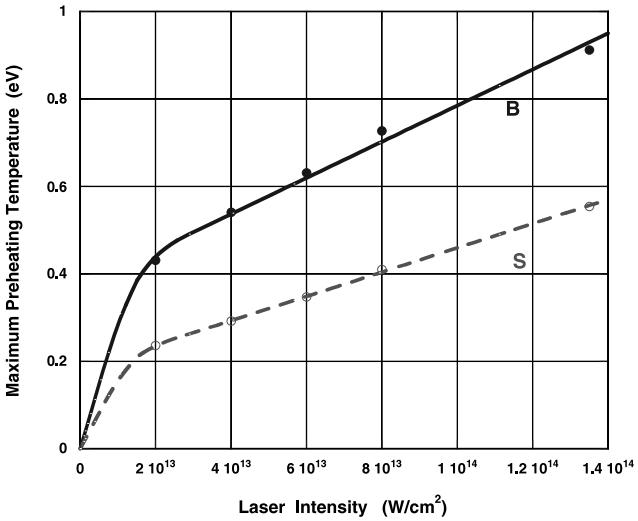

Fig. 3. The maximum value of the preheating temperature at the rear surfaces of base and step, 8 and 8.5 μm, as a function of laser intensity. The values are taken just before the respective shock breakouts.

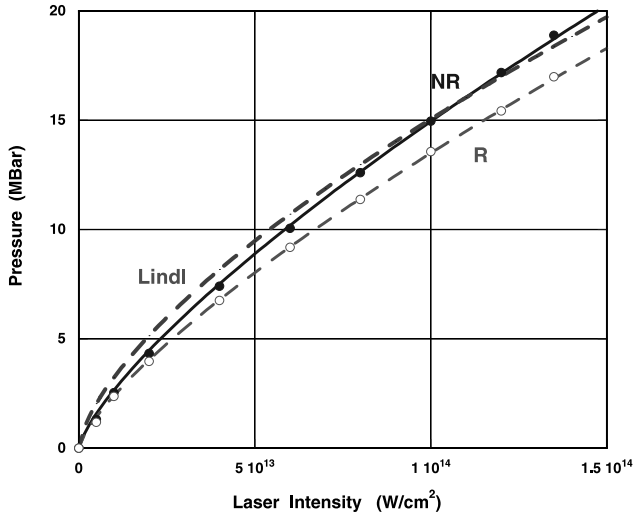

Fig. 5. Shock pressure in Al step target for radiative and non-radiative medium, using the code MULTI. Also shown the comparison with Lind's analytical formula.

integrated expansion from time zero up to shock breakout. Notice the fact that the step expansion is larger than that of the base. Indeed, in spite of a lower X-ray flux due to absorption in the step, the step rear side has more time available for expansion before the shock breakout.

The variations of the shock transit time in the step (the quantity that is measured in the experiments), between a purely hydrodynamical case and a radiative case, depend on a delicate balance of various factors.

Figure 5 shows the shock pressure as a function of laser intensity in the radiative and non-radiative cases. Here, for each laser intensity, we have drawn the maximum (in space and time) shock pressure in the step; however, since the shock wave is stationary in the step thickness, that is, its velocity is constant and so its pressure (apart from small fluctuations and reading errors) the choice is not critical.

The plot shows also the curve obtained with Lindl's (1995) scaling law, according to which $P = 8.6\ (I/\lambda)^{2/3}\ (A/2Z)^{1/3}$, *where* I is in units of 10^{14} W/cm^2 and λ in μm, to be compared with the non-radiative curve provided by the code. The pressure in the radiative case is decreased because a part of the laser beam energy is lost in the process of X-ray generation. The scaling for non-radiative and radiative medium are $4.73 \times 10^{-10}\ I^{0.75}$ and $4.27 \times 10^{-10}\ I^{0.75}$, respectively. These values have been obtained for 0.44 μm laser wavelength in the simulations. The obtained scaling is in agreement with what reported in (Batani *et al.*, 2003*c*) and obtained using the same laser system.

Figure 6 shows the shock transit time in the step as a function of laser intensity for the radiative (R) and non-radiative (NR) cases. The shock transit time is always longer in the radiative case (in our range of experimental parameters of laser intensity and target thicknesses). Several causes contribute to such effect. First of all, as seen in Figure 5, the shock pressure is smaller in the radiative case implying a smaller shock velocity and a longer transit time.

Second, the expansion causes a variation of the apparent step thickness, as well as a variation of shock velocity in the reduced-density medium. To check the relative importance of such effects, we have drawn the curves C and D in Figure 6. Curve C gives the results of non-radiative simulations using for a given laser intensity the *reduced* pressures corresponding to the *radiative* case (that is, the pressure obtained from curve R in Figure 5). If the increase in time was due to a reduction of pressure only, curve C should practically coincide with curve R (*radiative* results).

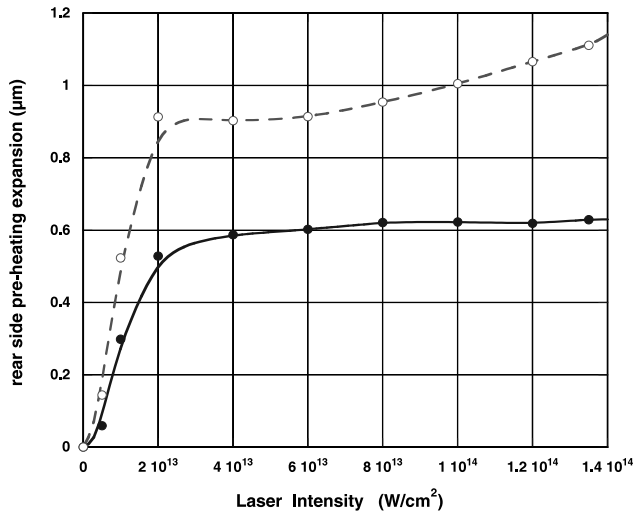

Fig. 4. Maximum preheating expansion of the rear surfaces of Al base and step as a function of laser intensity. Expansion is measured just before the respective shock breakouts. Interpolation curves are just visual guides for the eye.

https://doi.org/10.1017/S0263034607070048 Published online by Cambridge University Press

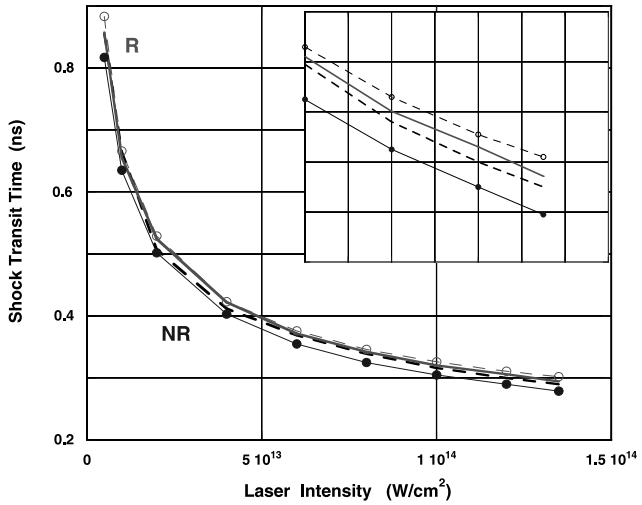

Fig. 6. Shock transit time in a 8.5 μm Al step for radiative (R) and non-radiative (NR) cases as a function of laser intensity. The curve C corresponds to the shock transit time obtained in the non-radiative case when a reduction of the pressure according to the radiative case is adopted (see Fig. 5). Curve D is obtained scaling the non-radiative values by the square root of the non-radiative and radiative pressures ratio. The inset on top-right shows the detail at high laser intensities.

Similarly, curve D is obtained by considering the *reduced* pressures corresponding to the *radiative* case; however instead of running a new simulation, we have simply assumed a square root dependence of D vs. P. Such dependence is exact for a perfect gas but, in our pressure range, also describes the behavior of Al quite well (see Figure 9a). In this case the shock transit time can then be obtained as $\Delta t_D = \Delta t_{NR} \cdot (P_{NonRad}/P_{Rad})^{1/2}$, where D and NR refers to the two curves in Figure 6, and P_{NonRad} and P_{Rad} are taken from Figure 5. As expected, curves D and C are very close to each other. Both curves represent the effect of pressure reduction only.

Instead, it is clear that curves C and D are quite different from curve R (*radiative* results). This shows that the reduction of shock pressure in the radiative case is one cause, but not the only one, for the increase of the shock transit time in the step. The remaining difference is due to preheating effects in Al, i.e. to induced expansion in the material at the rear sides of base and step. Such expansion affects the distance to be crossed by the shock as well as the average density of the propagation medium.

This effect was previously discussed in Honrubia *et al.* (1998, 1999) for planar Al targets. It globally brings to an increase in shock breakout times. Indeed expansion produces a reduction of average density of a layer of thickness Δx_o on the target rear side from ρ_o to ρ. This in turn produces an increase of the distance crossed by the shock of the order of $\Delta x \approx \Delta x_o\,(\rho_o/\rho)$ and an increase in shock velocity of the order of $D \approx D_o\,(\rho_o/\rho)^{1/2}$. Due to quadratic dependence of D over ρ the increase in lengths prevails, bringing to an increase in breakout time.

Now for a stepped target, we recall that the transit time is determined as $\Delta t = (t_s - t_b)$. If expansion at the base and step were equal, then such effect would disappear, bringing to no significant variation of the measured shock transit time (apart from the reduction of shock pressure due to X-ray generation). In our case instead, the expansion in the step is in sensibly larger than in the base (see Figure 4), the increase is larger for the step, bringing to longer transit times, as shown in Figure 6.

One critical question concerns the behavior of preheating effects at low laser intensities, as seen in Figure 6. We notice when the laser intensity on target is decreased, we have a strong reduction in X-ray conversion yield, bringing to a reduction of target preheating. Simultaneously longer time is needed by the shock to cross the target. This may result in no visible reduction of preheating effects when laser intensity is decreased.

Figure 7 shows the differences between curves R and NR of Figure 6: the curve labeled T refers to the total *normalized* change in shock transit time between the radiative and non-radiative cases, that is, to the quantity $(t_R - t_{NR})/t_{NR}$, where the curve symbols R, NR, and D are the same as defined in Figure 6. The curves P and E represents, respectively, the quantities $(t_R - t_D)/t_{NR}$ and $(t_D - t_{NR})/t_{NR}$, that is, they give respectively the relative weight of pressure reduction and preheating expansion. Let's notice that since P_{Rad} and P_{nonRad} shows the same scaling ($\sim I^{0.75}$), and since $\Delta t_D = \Delta t_{NR} \cdot (P_{NonRad}/P_{Rad})^{1/2}$, then the relative contribution coming from pressure reduction is constant.

In principle, we do expect that preheating effects to vanish going to sufficiently low laser intensities. This is indeed what happens for intensities larger than 10^{12} W/cm^2: we see that the shock transit time (curve T) decreases as the laser intensity decreases. This is the difference between the radiative shock transit time and the non-radiative one, normalized to the value of the non-radiative shock transit time. This means that, as expected, the preheating effect reduces

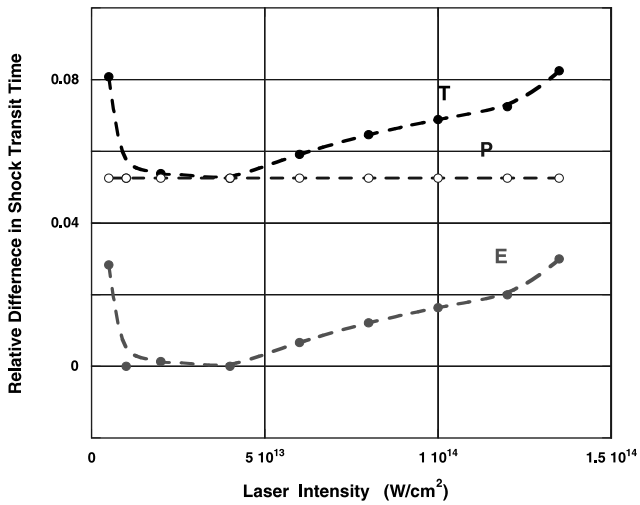

Fig. 7. Total relative (T) increase of the shock transit time vs. laser intensity and relative contributions of pressure reduction (P) and preheating expansion (E).

https://doi.org/10.1017/S0263034607070048 Published online by Cambridge University Press

and gradually the radiative transit times tend to be equal to the non-radiative one. The contribution due to expansion gradually vanishes and we only have remaining contribution from pressure reduction.

Using the code MULTI at very low laser intensities gave however the unexpected result shown in Figure 7. Indeed at $I = 10^{13}$ W/cm^2, the situation is surprisingly reversed and the normalized transit time increases again.

This result very likely depends on the fact that at low laser intensities both the process of X-ray generation (described in a simple multi-group approach using some opacity model) and the response of target material to heating and shock compression become highly questionable. For instance, the process of shock induced melting and evaporation are not well described by "*usual*" models such as the SESAME tables, at very low shock pressures, or in other words, extending our results to very low laser intensities (10^{12} W/cm^2 or below) does require the inclusion of a lot of material and radiation physics which are really outside the scope of the present work. Moreover it is clear that simulations or experiments below 10^{12} W/cm^2 are not of any relevance to laser-driven shock-EOS studies. It is certainly true that at very low laser intensities, it is expected that the effects of preheat vanish since there is no significant generation of hard X-rays, and because heating of the target rear side below the evaporation (or even the melting) temperature is unable to cause any expansion of the target material on rear side.

In order to complete the discussion, let's look at the graph in Figure 8. This is a schematic qualitative drawing of the phase diagram of Al in an arbitrary-units bi-log plot. From Al data, we know that the melting temperature is 900 K at standard pressure, while it is 5200 K along the Hugoniot curve of Al (at 1.2 Mbar). This temperature is much larger than the boiling temperature at standard conditions (2500 K)

We must consider that just after shock breakout, a rarefaction wave is reflected back in the material, as described in this paper, and the material on target rear side unloads (virtually to zero pressure) lowering its temperature. Such an unloading curve can be calculated using SESAME or MPQeos. Now, the important point is that certainly all the states which have a shock temperature above 5200 K, will result in final states (unloaded points) which are above the liquid/gas transition, and therefore give raise to a density gradient on target rear side. Let's notice that in our conditions, a pressure of 1.2 Mbar corresponds to a laser intensity on target equal to about 2×10^{12} W/cm^2. As we said before, this is just the sign that, around 10^{12} W/cm^2, Hydrodynamics codes need the inclusion of important details on the atomic physics in order to give reliable results.

A final question, in order to conclude the discussion on the effects of preheating, concerns the behavior of the shock velocity in the bulk, where the material is not free to expand due to the confinement by the surrounding material.

From Figure 9 we can draw several conclusions. First, the dependence of shock velocity on temperature along isochoric and isothermal curves is present, but very weak (usually preheating temperature are at most on the order of 1 eV). This shows indeed that if we have a material which is preheated but didn't expand, the shock velocity is practically the same as in the cold *standard* material. Again, this means that the preheating effects on shock propagation are mainly concentrated at the target rear layer, which can expand in vacuum reducing its density. All remaining dependencies can be understood, at least qualitatively, on the basis of the simple square root scaling $D \approx (P/\rho_o)^{1/2}$. This strictly holds for perfect gases, that is, in the limit of large temperatures and/or of large shock pressures. At very low preheating temperatures and shock pressures (i.e. when shocks are becoming weak and approaching a sound wave) dependencies are more complicated, reflecting the complexity of solid-state physics.

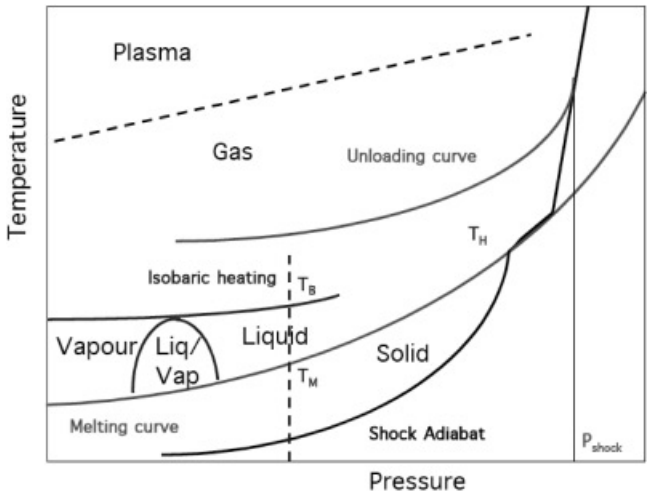

Fig. 8. (Qualitative) phase space of Al showing the various transformations. Here $T_M \sim 900$ K is the melting temperature at standard pressure; $T_B \sim 2500$ K is the boiling temperature at standard pressure; $T_H \sim 5200$ K is the melting temperature along the Hugoniot curve of the material (shock adiabat). Shock compression at pressure P_{shock} may induce direct passage to the gas/plasma phase, or it can produce temperatures equal to or larger than T_H. In this case unloading (relaxation) of the material to virtual zero pressure may bring to a final state above the liquid/gas transition line, thereby producing an appreciable expansion on rear side. Similarly preheating above T_B will induce change to the gas phase.

CONCLUSIONS

In this paper, we showed the results of simulations devoted to study the behavior of Al as a reference material for laser driven EOS experiments. X-radiation generated during the laser interaction with the Al base material leads to the reduction of shock pressure. This implies increase in shock transit time in the step target. X-ray preheating leads to the expansion of the target rear surfaces. Under typical experimental conditions (Batani *et al.*, 2004), this brings to an increase of the measured shock transit time, i.e. to a decrease of the *measured* shock wave velocity. The effect becomes larger at higher laser intensities.

https://doi.org/10.1017/S0263034607070048 Published online by Cambridge University Press

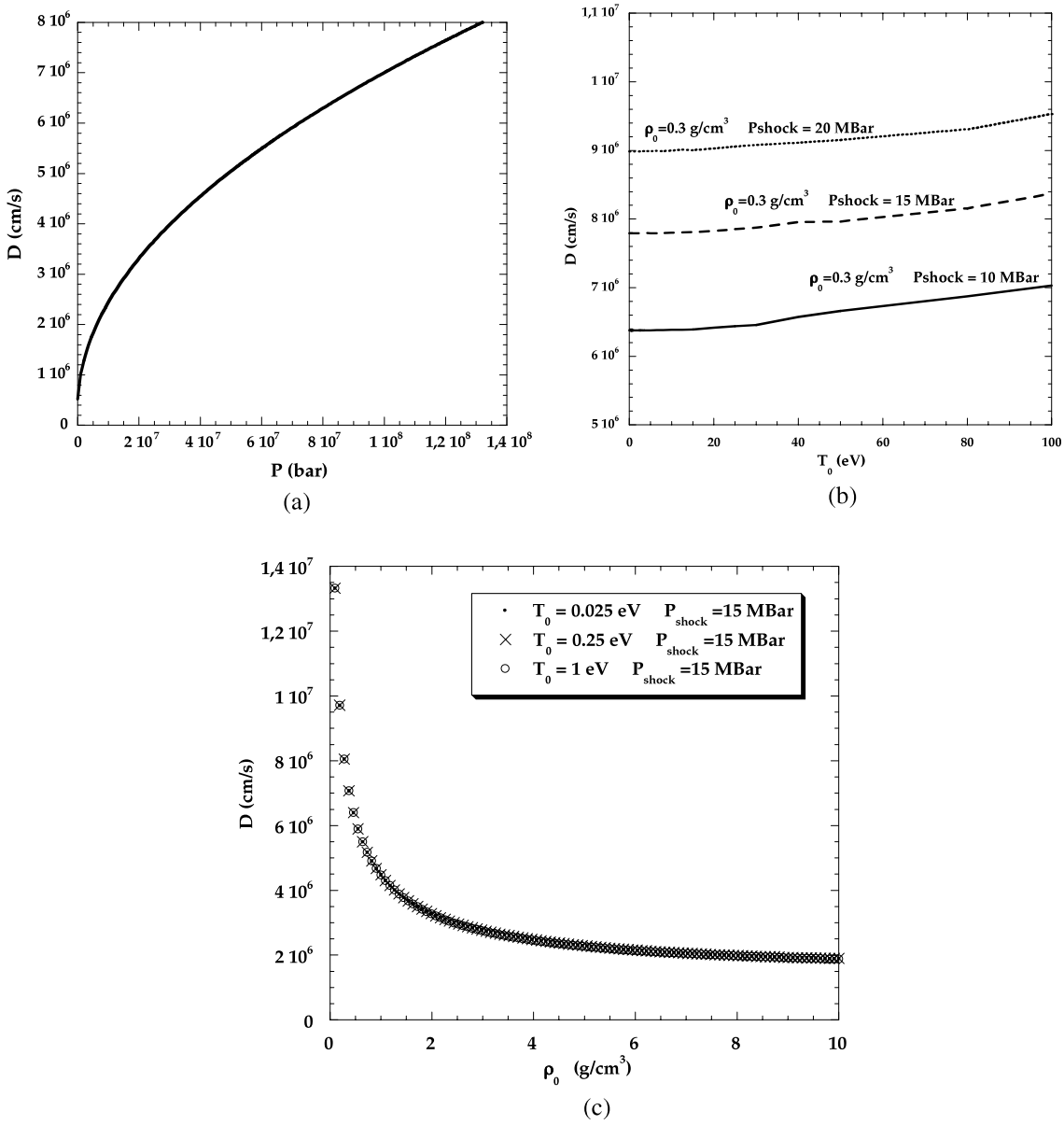

Fig. 9. Change in the shock velocity in Al (deduced from SESAME EOS tables): along the Hugoniot curve (**a**) for a material initially in normal conditions (ρ_o = m2.7 g/cm^3, T = 0.025 eV); along isochoric curves, that is, for constant density ρ_o = 0 .3 g/cm^3 (**b**); along isothermal curves, that is, for constant initial temperatures (**c**). Notice the very weak dependence on initial temperature for the behavior of shock velocity vs. initial density along isothermal curves (Fig. 9c).

ACKNOWLEDGMENTS

We acknowledge Rafael Ramis and Javier Honrubia (Universidad Politecnica, Madrid, Spain) for very useful discussions. One of the authors (TD) would like to thank the staff of ETSII of the Universidad Politecnica for their hospitality during her stay in Madrid. This work has been partially supported by the grant SAB2002-0174 of the Spanish Ministry of Education and project FTN2003-6901 of the Spanish Ministry for Science and Technology, by the COST action P14 "ULTRA" and by the TRIL program, ICTP, Trieste, Italy.

REFERENCES

Al'tshuler, L.V., Krupnikov, K.K. & Brazhnik, M.I. (1958). Dynamic compressibility of metals under pressures from 400,000 to 4,000,000 atmospheres. *Soviet JETP* **34**, 614.

Batani, D., Balducci, A., Beretta, D. & Bernardinello, A., Lower, Th., Koenig, M., Benuzzi, A., Faral, B. & Hall, T. (2000). Equation of state data for gold in the pressure range $<$ 10 TPa. *Phys. Rev. B* **61**, 9287.

Batani, D., Bleu, C. & Lower, Th. (2002). Modelistic, simulation and application of phase plates. *Euro. Phy. J. D* **19**, 231.

https://doi.org/10.1017/S0263034607070048 Published online by Cambridge University Press

Batani, D., Bossi, S., Benuzzi, A., Koenig, M., Faral, B., Boudenne, J.M., Grandjouan, N., Temporal, M. & Atzeni, S. (1996). Optical smoothing for shock wave generation: Application to the measurement of equation of state. *Laser Part. Beams* **14**, 211.

Batani, D., Löwer, Th., Hall, T., Benuzzi, A. & Koenig, M. (2003*b*). Production of high quality shocks for equation of state experiments. *Euro. Phy. J. D* **23**, 99.

Batani, D., Stabile, H., Ravasio, A., Desai, T., Lucchini, G., Ullschmied, J., Krousky, E., Skala, J., Kralikova, B., Pfeifer, M., Kadlec, C., Mocek, T., Prg, A., Nishimura, H., Ochi, Y. & Zvorykin, V. (2003*a*). Shock pressure induced by 0.44 μm laser radiation on aluminum. *Laser Part. Beams* **21**, 479.

Batani, D., Stabile, H., Ravasio, A., Desai, T., Lucchini, G., Ullschmied, J., Krousky, E., Juha, L., Skala, J., Kralikova, B., Pfeifer, M., Kadlec, C., Mocek, T., Präg, A., Nishimura, H. & Ochi, Y. (2003*c*). Ablation pressure scaling at short laser wavelength. *Phys. Rev. E* **68**, 067403.

Batani, D., Stabile. H., Tomasini, M., Lucchini, G., Ravasio, A., Koenig, M., Benuzzi-Mounaix, A., Nishimura, H., Ochi, Y., Ullschmied, J., Skala, J., Kralikova, B., Pfeifer, M., Kadlec, Ch., Mocek, T., Präg, A., Hall, T., Milani, P., Barborini, E. & Piseri, P. (2004). Hugoniot data for carbon at megabar pressures. *Phys. Rev. Lett.* **92**, 065503.

Benuzzi, A., Koenig, M., Faral, B., Krishnan, J., Pisani, F., Batani, D., Bossi, S., Beretta, D., Hall, T., Ellwi, S., Huller, S., Honrubia, J. & Grandjouan, N. (1998). Preheating study by reflectivity measurements in laser driven shocks. *Phys. Plasmas* **5**, 2410.

Eidmann, K. (1994). Radiation transport and atomic physics of Plasmas. *Laser Part. Beams* **12**, 22.

Honrubia, J.J., Dezulian, R., Batani, D., Bossi, S., Koenig, M., Benuzzi, A. & Grandjouan, N. (1998). Simulation of preheating effects in shock wave experiments. *Laser Part. Beams* **16**, 13.

Honrubia, J.J., Dezulian, R., Batani, D., Koenig, M., Benuzzi, A., Krishnan, J., Faral, B., Hall, T. & Ellwi, S. (1999). Preheating effects in laser driven shock waves. *J. Quant. Spectroscopy Radia. Transf.* **61**, 647.

Kemp, A.J. & Meyer-ter-Vehn, J. (1998). An equation of state code for hot dense matter based on the QEOS description. *Nucl. Instr. Meth. Phys. Res. A* **415**, 674.

Koenig, M., Faral, B., Boudenne, J.M., Batani, D., Bossi, S. & Benuzzi, A. (1994). Use of optical smoothing techniques for shock wave generation in laser produced plasmas. *Phys. Rev. E* **50**, R3314.

Koenig, M., Faral, B., Boudenne, J.M., Batani, D., Bossi, S., Benuzzi, A., Remond, C., Perrine, J., Temporal, M. & Atzeni, S. (1995). Relative consistency of equation of state by laser driven shock waves. *Phys. Rev. Lett.* **74**, 2260.

Lindl, J. (1995). Development of the indirect-drive approach to inertial confinement fusion and the target physics basis for ignition and gain. *Phys. Plasmas* **2**, 3933.

Lyon, D.P. & Johnson, J.D., Eds. (1992). SESAME: The LANL Equation of State Database. Report No. LA-UR-92-3407. Los Alamos, NM: Los Alamos National Laboratory.

More, R.M., Warren, K.H., Young, D.A. & Zimmerman, G.B. (1988). A new quotidian equation of state (QEOS) for hot dense matter. *Phys. Fluids* **31**, 3059.

Ramis, R., Schmalz, R.F. & Meyer-ter-Vehn, J. (1988). MULTI: A computer code for one-dimensional multigroup radiation hydrodynamics. *Comput. Phys. Commun.* **49**, 475.

Zeldovich, Ya.B. & Raizer, Yu.P. (1967). *Physics of Shock Waves and High Temperature Hydrodynamic Phenomena*. New York: Academic Press.

https://doi.org/10.1017/S0263034607070048 Published online by Cambridge University Press